Journal of Animal and Veterinary Advances 12 (19): 1512-1523, 2013
ISSN: 1680-5593
© Medwell Journals, 2013

Biophysical Regulation of Net Ecosystem Carbon Dioxide Exchange over an Artificial Pasture in the Three-River Source Region of the Qinghai-Tibetan Plateau

[1,2]Bin Wang, [1]Jie Li, [3]Liang Zhao, [3]Shixiao Xu,
[4]Yanhong Tang, [5]Mingyuan Du and [1]Song Gu
[1]College of Life Science, Nankai University, Tianjin, China
[2]College of Life Science and Agriculture and Forestry,
Qiqihar University, Qiqihar, China
[3]Chinese Academy of Sciences,
Northwest Plateau Institute of Biology, Xining, China
[4]National Institute for Environmental Studies, Tsukuba, Japan
[5]National Institute for Agro-Environmental Sciences, Tsukuba, Japan

Abstract: Measurements of Net Ecosystem CO_2 Exchange (NEE) were made, using eddy covariance to investigate the biophysical regulation of an *Elymus nutans* artificial pasture in the Three-River Source Region on the Qinghai-Tibetan Plateau during 2008. The hourly maximum rates of NEE was -7.89 μmol CO_2/m^2/sec (negative values representing net carbon uptake). The maximum daily NEE for the pasture was -2.91 g/cm^2/day. The annual NEE sums in pasture was 140.01 g cm^2/year. For the entire growing period, the light response curves of daytime NEE showed a medium apparent quantum yield (α = -0.0275 μmol μmol^{-1}). However, the α values varied with varied with canopy development, air temperature (T_a) and Soil Water Content (SWC) and Vapor Pressure Deficit (VPD). Piecewise regression results suggested that the optimal T_a and VPD for hourly daytime NEE were 14.1°C and 0.65 kPa, respectively. During the entire growing period, the daytime NEE decreased as the SWC increased. The apparent temperature sensitivities of ecosystem respiration (Q_{10}) was 3.0 for the entire growing season and it was significantly controlled by soil moisture. During the growing season, the leaf area index explained approximately 32.5% of the variation in daily NEE.

Key words: Net ecosystem CO_2 exchange, ecosystem respiration, artificial pasture, *Elymus nutans*, eddy covariance, The Three-River Source Region

INTRODUCTION

The grassland ecosystem occupies approximately 1/3 of the total global land area and it is an important component of the earth's carbon circulation (Adams *et al*., 1990). For the past few decades, ecologists have studied the effect of environmental factors (such as radiation, temperature, water and soil nutrition), biological factors and management measures on the carbon exchange between the land surface and the atmosphere of the grassland ecosystem by using eddy covariance, (McFadden *et al*., 2003; Novick *et al*., 2004; Kato *et al*., 2004) and they noted the significance of human activity on carbon exchange process (Wohlfahrt *et al*., 2008). The grassland of China occupies approximately 40% of the nation's total land area and it plays a very important role in the regional circulation of carbon (Fu *et al*., 2009). However, because the study of China's grassland carbon flux started late, carbon process studies have mainly been focused on low-lying regions (Hao *et al*., 2006; Yu and Sun, 2006).

The Qinghai-Tibetan Plateau has drawn a lot of attention as the "initiation zone" and the "sensitivity zone" for China's weather changes (Feng *et al*., 1998). Although, there have been reports on the carbon exchange between the land surface and the atmosphere and the driving mechanism underlying the primary natural vegetation types (e.g., alpine meadows and alpine shrubs) over the last few years (Li *et al*., 2005; Shi *et al*., 2006; Saito *et al*., 2009), there have only been a few reports on the carbon exchange process, source/sink function for artificial vegetation (e.g., artificial grassland) and the driving mechanism of environmental and biological factors.

The Three-River Source Region (TRSR; i.e., the source of the Yangtze, Yellow and Mekong rivers, well

Corresponding Author: Song Gu, College of Life Science, Nankai University, Tianjin, China

known as the "water tower of Asia", located in the hinterland of the Qinghai-Tibetan Plateau) is located in the hinterlands of the QingHai-Tibet Plateau. In recent years, the grassland in the region has degraded to a serious extent. Statistics indicate that the area that is experiencing moderate and severe degradation has already reached 5.7×10^6 hm^2, occupying 55.40% of the total usable grassland area (Chen, 2005). To curb grassland degradation in the region, the Chinese government has established a large artificial grassland in the Three-River Source Region. By 2005, the artificial grassland area had already reached 160,000 km^2 (Wang *et al*., 2005). Establishing artificial grassland on a degraded alpine meadow ecosystem can improve the productivity of the original ecosystem, increase the organic carbon content of the soil and speed up the turnover rate of the soil's nutrients to alleviate the grassland degradation trend in the region (Wu *et al*., 2010). Researchers sought to identify the impact of the implementation of artificial grassland on the ecosystem's carbon budget. Researchers wanted to know how environmental and biological factors can change the carbon budget of the artificial grassland but there are few reports on these issues. Therefore, this study used continuous observation data from an eddy covariance system from January 1st 2008 to December 31st and researchers performed a quantitative analysis of the CO_2 flux variations and controlling factors of the pasture in TRSR to achieve the following objectives: quantify the magnitude of CO_2 exchange; investigate the biophysical regulations on CO_2 flux and calculate the carbon balance in 2008 over the pasture.

MATERIALS AND METHODS

Study site: The study region is located in the GeDuo pastoral committee grass field, 25 km Southeast of Dawu town, GuoLuo prefecture, QingHai Province which is located at TRSR. Its geological coordinates are 100°26'-100°41'E, 34°17'-34°25'N with an elevation of 3980 masl. The region has typical plateau continental weather, the annual average sunshine is 2576 h, the radiation is strong without absolute frost and the annual average temperature is -0.5°C. The monthly average temperature is -12.7°C, the average temperature in July is 9.8°C and the annual precipitation volume is approximately 500 mm with 85% of the precipitation concentrated between May and September. The soil types are mainly alpine meadow soil and alpine shrub soil. The artificial pasture was established in May 2002 and the total area is 2000 hm^2. It was single-sowed with *Elymus nutans* and the vegetation height is 40~60 cm. The meadow was grazed in winter and the grazing intensity was medium.

Eddy flux and micrometeorological measurements: The 3 m high meteorological observation towers supporting the measuring system was installed at the center of the observation field. CO_2 and H_2O fluxes were measured using the Eddy Covariance Method. The uniform fetch was >300 m from the tower in all directions. A 3 dimension ultrasound wind-speed meter (CSAT-3; Campbell Scientific Inc. (CSI), Logan, UT, USA) was used to measure turbulence. Fluctuations in heat, CO_2 and water vapor density were measured using the anemometer temperature and an open-path CO_2/H_2O infrared gas analyzer (CS7500; CSI, USA) at 10 Hz. The average value was output once every 15 min and the data were saved in a data collection device (CR5000, CSI, USA). The CO_2/H_2O analyzer system was calibrated each year.

At the same time that researchers measured the CO_2 flux, researchers also performed measurements of other regular weather factors. The regular measurement system was installed on the same flux tower as the eddy measurement system. Among these measurements, the sun's radiation and net radiation flux measurement height was 150 cm as recorded by a net radiation meter (CNR-1; Kipp and Zonen, Delft, the Netherlands) and a photosynthetic photon flux density instrument (LI-190SB; Li-Cor, Lincoln, NE, USA). The soil temperature was measured using copper-constantan thermocouples (105-T; CSI, USA) and the measurement depths were 5, 10 and 30 cm underground. The air temperature and humidity were measured with a humidity and temperature probe (HUMP45C; CSI, USA) and the measurement heights were 110 and 300 cm above ground. The wind speed and direction were measured using cup anemometers (034A-L and 014A, R.M. Young Co., Traverse, MI, USA) and the measurement heights were 110 and 300 cm above ground. The soil heat flux was measured with heat flux plates (HFT-3; CSI, USA) and the measurement depth was 2 cm underground. Altogether, there were 3 heat flux plates in the sample field. The soil heat flux was the average value of the three heat flux plates. The soil moisture was measured using time-domain reflectometry sensors (CS615; CSI, USA) and the measurement depths were 5, 20 and 30 cm underground. The soil surface temperature was measured with thermometers (107; CSI, USA) at three points in a 1 m^2 area. The precipitation volume was measured using a tipping bucket (TE525MM; CSI, USA) and the measurement height was 70 cm above the ground. The output data were the average value for every 15 min. These data were stored in the data collector (CR5000; CSI, USA).

Data processing and energy balance closure: The data were obtained from January 1st, 2008 to December 31st, 2008. All micrometeorological and flux data went through data quality control. The raw flux data were preprocessed

before analysis which primarily included outlier exclusion (±3δ), dimensional coordinate rotation and Webb-Pearman-Leuning correction (Webb *et al*., 1980) among others.

The closure of the 15 min averaged surface energy budget was examined by performing an Ordinary Linear Regression (OLR) between the sum of eddy fluxes (LE+H) and the available energy (R_n-G) during all of 2008:

$$LE+H = 0.69\times(R_n-G)+22.06\ (r^2 = 0.84)$$

Where:

H and LE = The sensible and latent heat fluxes, respectively
R_n = The net radiation
G = The soil heat flux and all the flux values are daily averages (MJ/m^2)

Therefore, the energy closure rate is 69% for the sample field and this energy closure slope is inside the published energy closure range (0.55~0.90) (Wilson *et al*., 2002). It is notable that the area contributing to the flux is large, flat and wide open but the closure slope is relatively small. This difference might be caused by relatively low temperatures and wind speeds and further study will be needed to determine whether this is the reason for the discrepancy.

Because the flux observation and measurement are affected by the weather conditions in the wild, the data can be processed as follows: eliminate data during precipitation and during the morning dew time periods and eliminate data from the nights of the growing season when the carbon flux value is negative. The data from the night times when the friction wind velocity (U*)≤0.2 m sec^{-1} can be treated as invalid data because the turbulence intensity at that time is not strong enough for the device to properly record CO_2 flux data (Gu *et al*., 2003). After being processed, the usable flux data reached 67%.

The missing data could usually be interpolated based on the nonlinear empirical relation between the established carbon flux value and environmental factors.

The relationship between R_e (e.g., NEE in the whole days during the non-growing season and for the night time (photosynthetic photon flux density <10 μmol/m^2/sec) during the growing season) and soil temperature at 5 cm depth (T_s) was calculated by Van't Hoff equation (Eq. 1)) fitted to the 15 min nighttime 'available data' (Lloyd and Taylor, 1994). Then, Eq. 1 can be used to reverse-derive the ecosystem respiration during the day time (photosynthetic photon flux density >10 μmol/m^2/sec) during the growing season.

$$R_e = a\exp(bT_s) \quad (1)$$

Where:

R_e = The nighttime ecosystem respiration rate (μmol CO_2/m^2/sec)
T_s = The soil temperature at a depth of 5 cm
a and b = Fitted coefficients

The sensitivity coefficient of respiration for the ecosystem (Q_{10}) was derived from Eq. 2, representing the relative growth volume of the ecosystem respiration for every 10°C temperature increase as follows:

$$Q_{10} = \exp(10b) \quad (2)$$

For the day time during the growing season, a Michaelis-Menten rectangular hyperbola (Eq. 3) fitted to the 15 min daytime 'available data' (Falge *et al*., 2001):

$$F_c = \frac{F_{max}\alpha PPFD}{F_{max}+\alpha PPFD} \quad (3)$$

Where:

PPFD = The photosynthetic photon flux density (μmol/m^2/sec)
F_{max} = The value of NEE at a saturating light level (μmol CO_2/m^2/sec)
α = The apparent quantum yield
R_e = The ecosystem respiration

Aboveground biomass and leaf area index measurements: The biomass and leaf area index were measured 6 times over the whole growth season. The above ground biomass measurement adopted the harvesting method with five randomly installed samples. The sample size was 0.5×0.5 m and the vegetation was cut off with the root and brought back to the lab to be dried in a 65°C thermostatic oven. The leaf area index employed the leaf area meter measurement (LI-3100, Li-Cor). Based on the plant phenology data in TRSR, researchers assumed that the biomass and the leaf area index for the sampling field were both zero before April 20th and after October 18th. April 20th (DOY111) and October 18th (DOY292) were the start and end dates for the growing season. Measurements of LAI were linearly interpolated to daily intervals (Li *et al*., 2005).

RESULTS

Meteorological and biological factors: Figure 1a shows that the PPFD peaks occurred during the season between May and August when the solar elevation angle was higher. Because of the high elevation, the PPFD values for the plateau were higher and the maximum daily values could reach 695.9 μmol/m^2/sec. Vapor Pressure Deficit

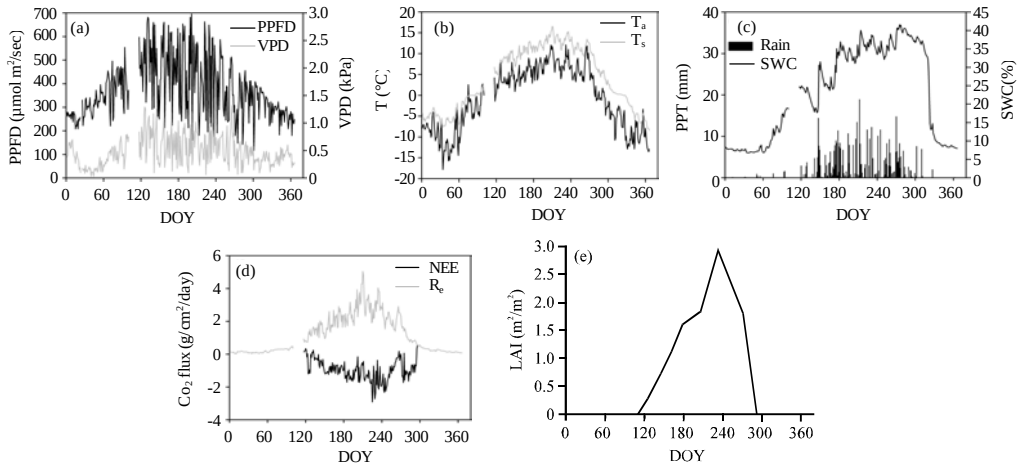

Fig. 1: Temporal variations of a) Photosynthetic Photon Flux Density (PPFD) and Vapor Pressure Deficit (VPD); b) daily mean air temperature (T_a) and soil temperature at a depth of 5 cm (T_s); c) daily precipitation (PPT) and Soil Water Content at 5 cm depth (SWC); d) daily Net Ecosystem CO_2 Exchange (NEE) and ecosystem respiration (R_e) and e) Leaf Area Index (LAI) during 2008

(VPD) also showed significant seasonal variations. VPD reached its highest value (approximately 1.32 kPa) during the growing season and its lowest value (approximately 0.04 kPa) during the winter (Fig. 1a). The daily mean air temperatures (T_a) and soil temperatures at a depth of 5 cm (T_s) had the same seasonal variation trends and the daily average value variations in T_a and T_s were -17.8~12.1°C and -8.4~16.5°C. The annual average T_a was -0.54°C and the T_s annual average temperature was 4.2°C (Fig. 1b). The annual precipitation (PPT) was 628.9 mm which was higher than the average precipitation across multiple years (approximately 500 mm) and the precipitation during the May to September period made up 66.4% of the annual precipitation (Fig. 1c). Soil Water Content (SWC) variation was strongly dependent on the PPT, SWC was higher from May to October and it was generally maintained above 20% (Fig. 1c).

Figure 1e shows that Leaf Area Index (LAI) for the pasture sampling field started to increase at the end of April and the maximum was reached at the end of August (the maximum LAI was 2.9±0.3). In September, LAI decreased rapidly because of leaf aging. The growing season for the pasture in 2008 (DOY 113-292) could be divided into four stages (Table 1), that is, the early growing stage (I, DOY 113-145), the rapid growing stage (II, DOY 146-194), the peak growing stage (III, DOY 195-252) and senescence (IV, DOY 253-292).

Diurnal courses of carbon dioxide exchange: Figure 2d shows that the NEE daily variation is regular during every growth stage and it can be reflected as a daytime absorption and nighttime emission. In the morning, the NEE was converted from a positive value (representing carbon emission) to a negative value (representing carbon absorption) and before noon (10:00~11:00), the absorption value reached its maximum then the absorption value started to diminish. Around the evening (approximately 19:00), the NEE turned from a negative value to a positive value. The hourly maximum and minimum rates of NEE all occurred during the peak growing stage and they were 3.25 and -7.89 μmol $CO_2/m^2/sec$, respectively. Figure 2e shows that the hourly maximum rates of R_e for the pasture occurred at approximately 16:00 during the peak growing stage which was 5.03 μmol $CO_2/m^2/sec$.

Seasonal courses of carbon dioxide exchange: Figure 1d shows that from January to the end of April, the pasture NEE was longer than 0 because the above ground vegetation had withered thus the ecosystem was exhibiting carbon emissions (NEE>0). Starting from May 1st (DOY121), NEE began to be <0. The pasture ecosystem converted from carbon emission to carbon absorption (NEE<0) and it reached peak carbon absorption between July and August. Starting in September as the vegetation aged, the carbon absorption capability of the pasture gradually degraded. Starting at the end of October, the NEE began to be longer than 0 and the pasture ecosystem engaged in carbon emission (NEE>0). The maximum daily absorption value occurred on August 12th (DOY225) with -2.91 $g/cm^2/day$. The annual NEE for the pasture in 2008 was -140.04 $g/cm^2/year$. Thus, the pasture was a carbon sink in 2008.

Figure 1e shows that from January to the end of March, R_e was a bit higher than 0 and the change was not

Table 1: Parameters describing features of the rectangular hyperbolic responses of daytime NEE to incident PPFD (Eq. 3)

Treatments	DOY	LAI (m^2/m^2)	SWC (%)	T_a (°C)	VPD (kPa)	α (μmol μmol^{-1})	F_{max} (μmol CO_2/ m^2/sec)	R_e (μmol CO_2/ m^2/sec)	n	R^2	p-values
Early growing stage	113-145	0.35±0.06	22.88±3.59	4.02±1.86	0.52±0.29	-0.0022±0.0008	-5.22±0.34	0.21±0.04	16	0.93	<0.0001
Rapid growing stage	146-194	0.97±0.16	25.50±2.55	7.08±2.19	0.46±0.23	-0.0185±0.0053	-6.97±0.24	0.80±0.18	16	0.97	<0.0001
Peak growing stage	195-252	1.92±0.25	35.01±2.47	9.59±2.95	0.46±0.12	-0.0358±0.0091	-8.69±0.66	1.51±0.23	16	0.98	<0.0001
Senescence	253-292	1.38±0.35	37.03±3.63	7.32±1.16	0.56±0.23	-0.0122±0.0047	-6.95±0.53	0.66±0.12	16	0.96	<0.0001
Entire growing season	113-292	1.51±0.45	31.72±2.73	7.38±2.41	0.49±0.24	-0.0275±0.0048	-7.86±0.73	1.79±0.28	16	0.98	<0.0001
SWC≤25%						-0.0092±0.0022	-4.28±0.66	0.94±0.18	16	0.96	<0.0001
25%<SWC≤30%						-0.0258±0.0046	-5.81±0.82	1.59±0.22	16	0.98	<0.0001
SWC>30%						-0.0329±0.0058	-9.51±0.31	2.08±0.18	16	0.99	<0.0001
T_a≤5°C						-0.0220±0.0039	-5.89±0.41	1.25±0.16	16	0.97	<0.0001
5°C<T_a≤15°C						-0.0289±0.0202	-8.02±1.80	1.69±0.26	16	0.97	<0.0001
Ta>15°C						-0.0174±0.0054	-6.87±0.50	1.26±2.16	16	0.99	<0.0001
VPD ≤0.6 kPa						-0.0291±0.0058	-8.85±1.26	1.85±0.11	16	0.99	<0.0001
VPD>0.6 kPa						-0.0112±0.0045	-8.20±0.43	1.23±0.38	16	0.97	<0.0001

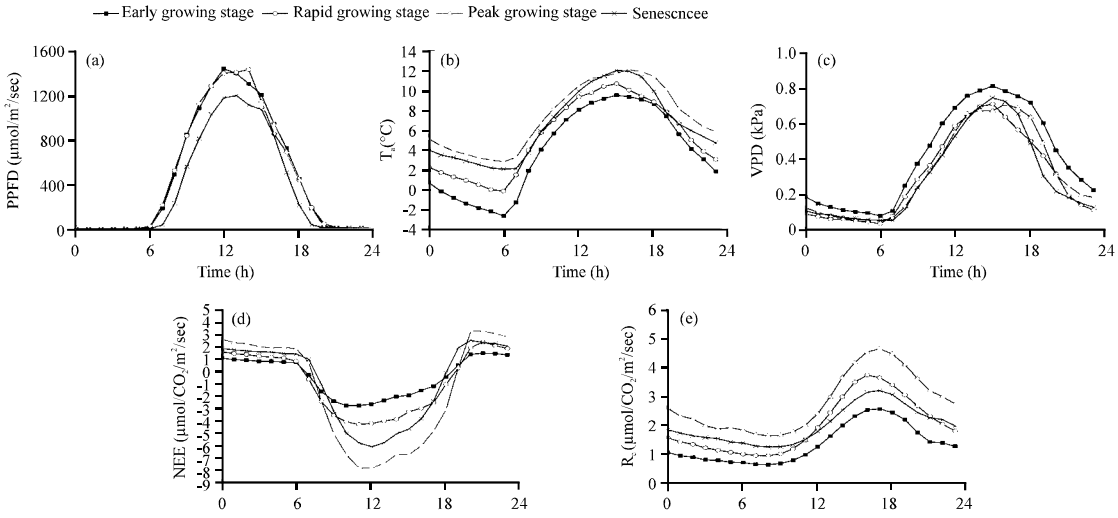

Fig. 2: Average diurnal cycles of a) Photosynthetic Photon Flux Density (PPFD); b) air temperature (T_a); c) Vapor Pressure Deficit (VPD); d) Net Ecosystem CO_2 Exchange (NEE) and e) ecosystem respiration (R_e) at different growing stages. Bars indicate±SE. Time of day is Beijing Standard Time (BST)

significant. Starting in April as the temperature rose, R_e started to rise. In 2008, the daily maximum R_e for the pasture was 5.04 g/cm^2/day which appeared on July 28th (DOY 210). The annual R_e was 403.57 g/cm^2/year in 2008.

Daytime NEE in response to PPFD: Researchers used Eq. 1 to depict the relationship between the daytime NEE and PPFD. The NEE data were averaged using PPFD bins of 100 μmol /m^2/sec. As shown in Fig. 3, when PPFD<1600 μmol/m^2/sec, the daytime NEE decreased as the PPFD increased. However, when PPFD>1600 μmol/m^2/sec, the daytime NEE increased as the PPFD increased (Fig. 3). Therefore, Eq. 1 is only valid for depicting the relationship between NEE and PPFD when PPFD<1600 μmol/m^2/sec. During the entire growing season, the model-derived quantum yield (α) and saturated NEE (F_{max}) in pasture developed as the canopy developed and the maximum values occurred during the peak growing stage with values of -0.0358 μmol/CO_2/μmol photons and -8.69 μmol/CO_2/m^2/sec, respectively (Table 1). During the entire growing season, the α and F_{max} in pasture were -0.0275 μmol/CO_2/μmol photons and -7.86 μmol/CO_2/m^2/sec, respectively.

To further study the impact of environmental factors on the NEE-PPFD curve, researchers inspected the NEE-PPFD curves under different T_a conditions (T_a≤5°C, 5°C<T_a≤15°C and T_a>15°C), different SWC conditions (SWC≤25%, 25%<SWC≤30% and SWC>30%) and different VPD conditions (VPD≤0.6 kPa, VPD>0.6 kPa). Under the micrometeorological conditions mentioned above, the NEE can be segmented again based on the PPFD (using 100 μmol/m^2/sec segments) and NEE was then averaged for each PPFD level. Statistically, this method can reduce or offset the errors that occurred during measurement (Falge *et al*., 2001).

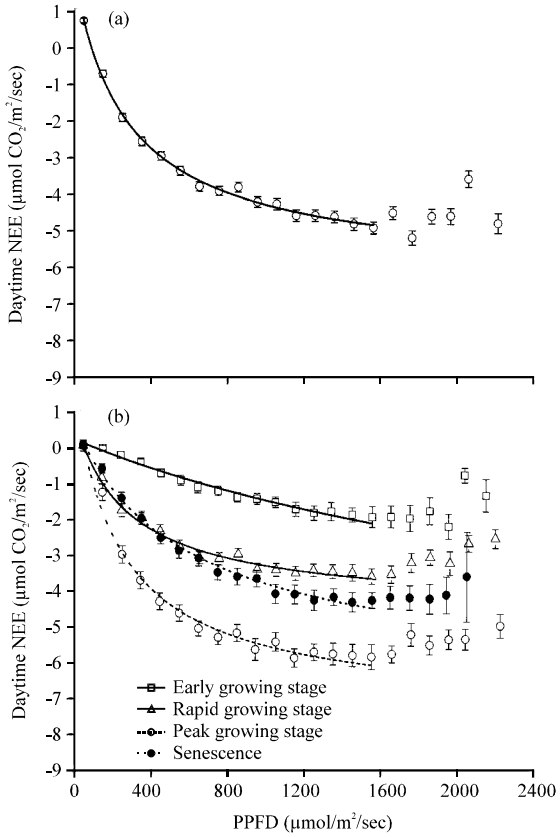

Fig. 3: Light response curves for a) the entire growing season and b) different growing stages. The daytime Net Ecosystem CO_2 Exchange (NEE) data were averaged with the PPFD bins at 100 μmol/m^2/sec. Bars indicate±SE. Equation 3 was used to fit the data when the PPFD was below 1,600 μmol/m^2/sec and the regression coefficients are presented in Table 1

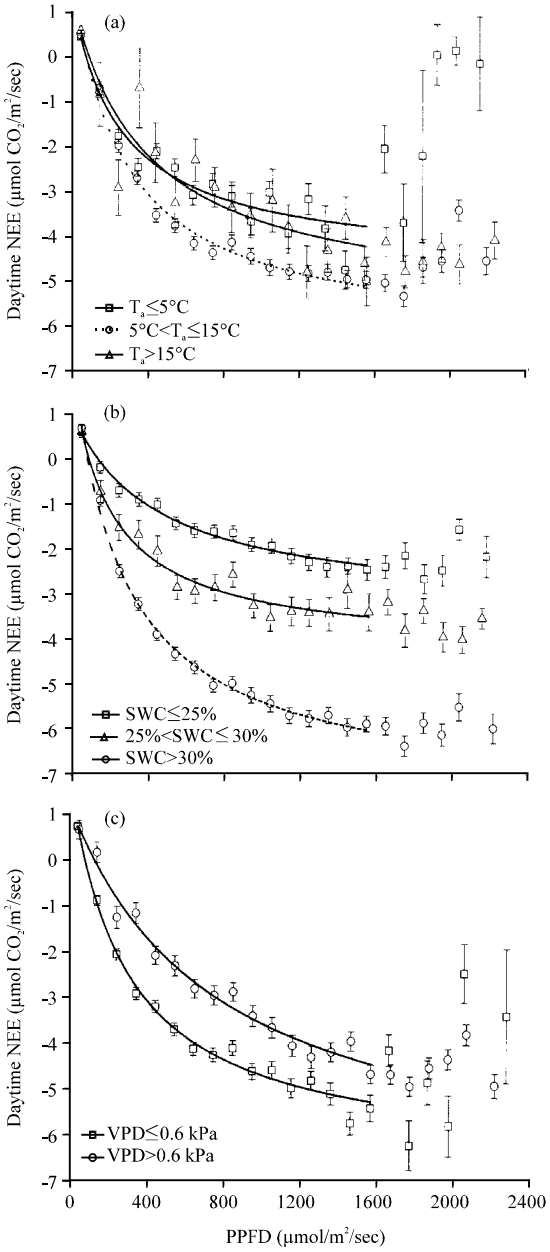

Fig. 4: Light response curves under a) different air temperatures (T_a); b) different Soil Water Contents (SWC) and c) different Vapor Pressure Deficit (VPD). The daytime Net Ecosystem CO_2 Exchange (NEE) data were averaged with the PPFD bins at 100 μmol/m^2/sec. Bars indicate±SE. Equation 3 was used to fit the data when the PPFD was below 1,600 μmol/m^2/sec and the regression coefficients are presented in Table 1

In the pasture, the F_{max} and α for the NEE-PPFD curve are under the influence of the SWC, T_a and VPD. The magnitudes of F_{max} and α increase as the SWC increases and at SWC<20%, F_{max} and α are significantly lower than they are when SWC>30%. F_{max} and α are highest when 5°C<T_a≤15°C. F_{max} and α decrease as VPD increases and when VPD>0.6 kPa, F_{max} and α are 93 and 38% of their values when VPD≤0.6 kPa (Fig. 4 and Table 1).

Daytime NEE in response to T_a, VPD and SWC: For statistical purposes, the daytime NEE data were averaged by environmental parameters into bins with bin widths of 1°C for T_a, 1% for SWC and 0.1 kPa for VPD over all the PPFD values. According to Fig. 5, the relationship between daytime NEE and T_a and VPD can be depicted by a quadratic function and the stepwise regression analysis results showed that the optimal T_a and VPD values for 15 min daytime NEE were 14.1°C and 0.65 kPa, respectively (Fig. 5a and b). The daytime NEE diminished as the SWC increased (Fig. 5c).

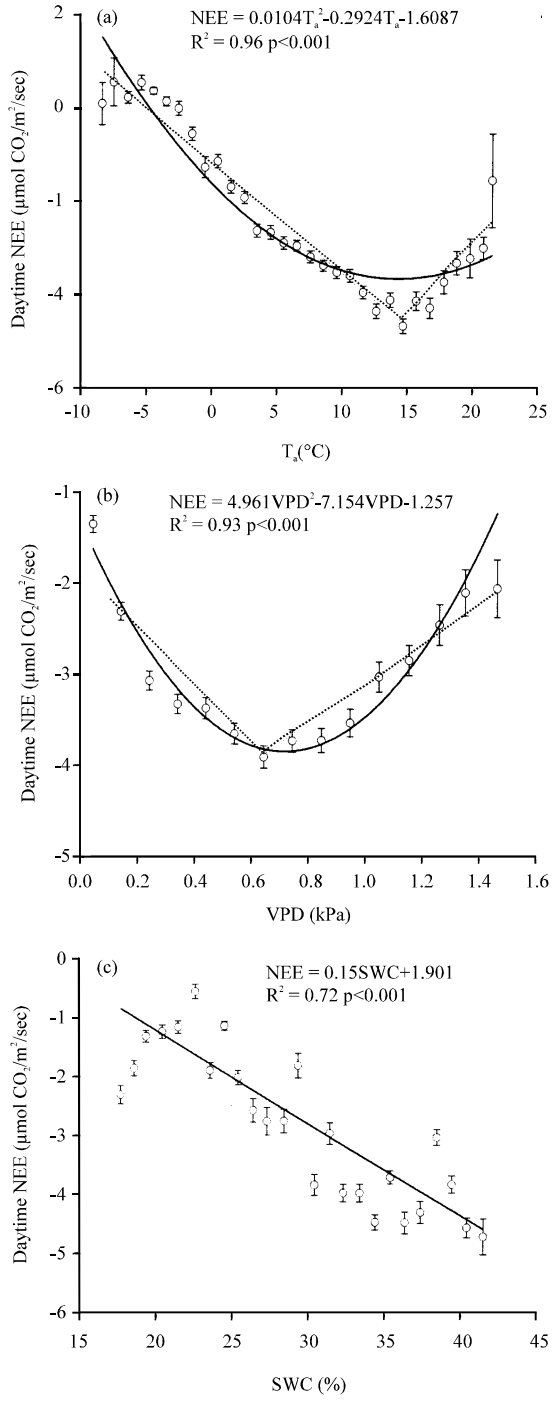

Fig. 5: Responses of daytime NEE to a) air temperate (T_a); b) Vapor Pressure Deficit (VPD) and c) Soil Water Content at 5 cm depth (SWC). The daytime NEE data were averaged with a bin width of 1 for T_a, 0.1 kPa for VPD and 1% for SWC, respectively. Bars indicate±SE. Solid lines were fitted by quadratic function fashion and dotted lines were fitted by a piecewise regression model in a and b

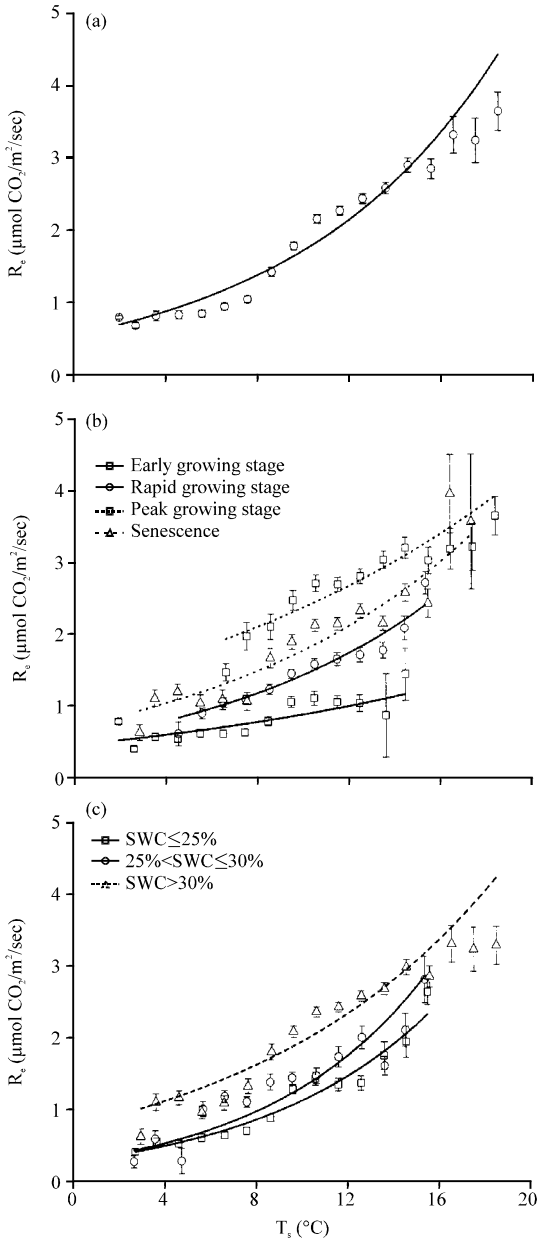

Fig. 6: Response of nighttime Net Ecosystem CO_2 Exchange (NEE) to change in soil temperature (T_s) for the a) entire growing season; b) different growing stages and c) different Soil Water Contents (SWC). The nighttime NEE data were averaged with a bin width of 1°C for T_s. Bars indicate±SE. Equation 1 was used to fit the data and the regression coefficients are presented in Table 2

R_e in response to T_s and SWC: For the entire growing season, the nighttime NEE data were bin averaged using T_s bins of 1°C. Figure 6 showed that R_e increased

Table 2: Regression coefficients as described in Eq. 1 and 2

Treatments	DOY	SWC	a	b	R^2	Q_{10}	p-values
Early growing stage	113-145	23.17±2.13	0.4661	0.0664	0.66	1.9425	<0.0001
Rapid growing stage	146-194	26.08±1.74	0.4809	0.1068	0.94	2.9096	<0.0001
Peak growing stage	195-252	35.62±2.23	1.2801	0.0583	0.83	1.7914	<0.0001
Senescence	253-292	37.63±3.02	0.6434	0.0992	0.89	2.6966	<0.0001
Entire growing season	113-292	32.41±2.25	0.5551	0.1088	0.95	2.9683	<0.0001
SWC≤25%			0.3136	0.1304	0.96	3.6840	<0.0001
25%<SWC≤30%			0.3188	0.1438	0.79	4.2123	<0.0001
SWC>30%			0.6936	0.0960	0.91	2.6117	<0.0001

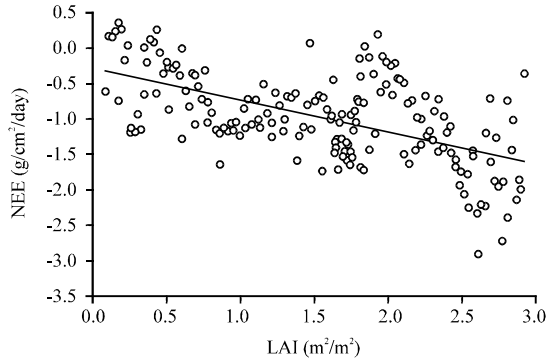

Fig. 7: The linear relationships between Leaf Area Index (LAI) and daily Net Ecosystem CO_2 Exchange (NEE) during the growing period from April 20 to October 18, 2008

exponentially as the temperature increased and the sensitivity coefficient of respiration for the pasture (Q_{10}) during the entire growth season was 3.0 (Table 2) and 1.9, 2.9, 1.8 and 2.7 for early, rapid, peak and senescence growing stages (Table 2), respectively.

To further investigate the impact of the SWC on T_s and R_e, researchers have investigated the T_s-R_e relation under different SWC conditions (SWC≤25%, 25%<SWC≤30% and SWC>30%). The results showed that the pasture's Q_{10} reached its maximum at 25%<SWC≤30% (Fig. 6 and Table 2).

Daily NEE in response to LAI: Figure 7 indicates that during the entire growth season, the pasture's daily integrated NEE and LAI had a linear relationship in which NEE = (-0.449±0.005)×LAI-(0.291±0.008), n = 175, adjusted r^2 = 0.325 and F = 84.8. Therefore, 32.5% of the NEE variation could be explained by the LAI variation.

DISCUSSION

Effects of biotic and abiotic variables on NEE: The maximum F_{max} for the pasture ecosystem occurred during the peak growing stage (-8.69 μmol/CO_2/m^2/sec) (Table 1) and it was very close to the F_{max} for a Steppe-Kobresia meadow during the peak growing season (-8.7 μmol/CO_2/m^2/sec) (Shi *et al*., 2006).

However, the value was lower than the maximum F_{max} for the other grassland ecosystems (from -9.6 to -40.2 μmol/CO_2/m^2/sec) (Li *et al*., 2005). During the entire growing season, the α of the pasture was 0.02754 which was higher than the α for the Steppe-Kobresia meadow on the Tibetan Plateau (-0.0159 μmol/CO_2/m^2/sec) (Shi *et al*., 2006). However, the α of the pasture for the entire growing period were at middle and low levels compared with those of other grassland and cropland ecosystems as reported by Li *et al*. (2005) (from -0.008 to -0.465 μmol/CO_2/μmol photons). These finding indicates that the light-use efficiency of the pasture was low. These data were related to the fact that the construction species for the pasture is C3 vegetation and that the pasture's ecosystem has high elevation and low temperatures (Zhao *et al*., 2008).

Under low T_a (T_a≤5), the F_{max} and α of the NEE-PPFD curve for the pasture are relatively low (Table 1) which main because the low temperature can suppress the activity of photosynthesis-related enzymes (Potvin *et al*., 1986). This situation was also found in the Inner Mongolian desert steppe (Yang *et al*., 2011). At SWC<20%, the F_{max} and α of the NEE-PPFD curve for the pasture are relatively low (Fig. 4b and Table 2), primarily because the low SWC can constrain plant growth. A similar situation also occurred in the steppe in Mongolia (Li *et al*., 2005). During the senescence, the F_{max} and α of the NEE-PPFD curve for the pasture decreased significantly. This finding is related to the fact that when the plant ages, the chlorophyll content is significantly reduced and the activity of photosynthesis-related enzymes is decreased (Kura-Hotta *et al*., 1987). This phenomenon also occurs in California grassland (Xu and Baldocchi, 2004).

The optimal temperature for the maximum 15 min daytime NEE in the pasture was 14.1°C which was very close to that of an alpine meadow (15°C) (Gu *et al*., 2005). The T_a had notable effects on the NEE in the study. The NEE decrease at lower temperatures is most likely caused by the slow growing rate during the early and late stages of the growth seasons while the depression of NEE at relatively higher temperatures could be ascribed primarily to enhanced respiration and depressed plant photosynthesis in response to high temperatures and high radiation (Fu *et al*., 2006).

In many ecosystems, moisture is an important factor that impacts the daytime NEE. The daytime NEE for the pasture dropped when the soil moisture increased (Fig. 5c). This trend indicated that increased soil moisture can improve the carbon absorption capability of the pasture. Similar results have been found in a Mongolian steppe (Li *et al*., 2005). Early studies demonstrated that the lack of moisture could result in the closure of plant stomata, further reducing the plant's CO_2 absorption. In addition, stomata closure also had a significant impact on the leaves. An increasing leaf temperature can enhance leaf photorespiration which further reduces CO_2 acquisition by the plants.

In this study, the daytime NEE and VPD on the pasture experienced a quadratic relation (Fig. 5) and similar results were observed on a temperate desert steppe (Yang *et al*., 2011). The daytime NEE suppressed by the high VPD could primarily be attributed to the physical cohesiveness between the temperature and the VPD (Fig. 2). Because this relation can affect the hydraulic status of plants and plant leaves, leading to leaf closure, it can affect the CO_2 acquisition by the plants (Souza *et al*., 2004).

The carbon exchange between the plants and the atmosphere is under the joint regulation of multiple environmental factors (such as the PPFD, T_a, SWC and VPD) thus it is hard to distinguish the specific impact on NEE by a single factor, especially between the T_a and VPD because the rising T_a is always associated with an increased VPD. Therefore, to study the response mechanisms to environmental factors and NEE in the future, both modeling and multivariate analysis should be leveraged.

Nighttime NEE responses to T_s and SWC: R_e is affected by multiple environmental factors and biological factors and T_s and SWC can be regarded as controls (Fang and Moncrieff, 2001; Hunt *et al*., 2002).

R_e represented a exponential function with increasing temperature (Fang and Moncrieff, 2001). During the entire growing season, the Q_{10} for the pasture was 3.0 (Fig. 6a and Table 2), it is higher than the Q_{10} value for low elevation grassland ecosystems around the world (2.1, Wang and Fang, 2007). Early studies show that the Q_{10} value for R_e decreases as the temperature increases (Zheng *et al*., 2009). The relatively high Q_{10} value for the pasture in TRSR could result from the low temperature on the plateau. Therefore, the study results show that in the context of global warming, the pasture in TRSR has relatively stronger carbon emission potential.

Q_{10} reaches its maximum under medium SWC (Fig. 6 and Table 2). This situation also occurred in a *Stipa krylovii* steppe (Wang *et al*., 2008). Under high SWC, the soil moisture can hinder the diffusion of O_2. Therefore, this factor can suppress the decomposition of organic matter and the microbial respiration rate. Under these conditions, the CO_2 release and temperature are not sensitive and the Q_{10} value is relatively low (Davidson *et al*., 2000; Jia *et al*., 2007). However, under low SWC, the primary component composed of R_e comes from the more recalcitrant carbon material which has a low Q_{10} (Raich and Schlesinger, 1992; Reichstein *et al*., 2002). The situations discussed above cannot explain the high Q_{10} value at senescence (Q_{10} = 2.7, SWC>30%) (Table 2). In the pasture ecosystem Q_{10} depends not only on soil water conditions but also on phenological stage of plant growth. A similar situation also occurred in the Inner Mongolian desert steppe (Yang *et al*., 2011).

The effect of LAI on daily NEE: The structure of the plant canopy, especially the leaf area and light interception capability, determine the quantity of radiation power absorbed and reflected by the plant canopy. Therefore, these factors can have a direct impact on plant photosynthesis (Ogren, 1993; Baldocchi and Harley, 1995). For the pasture ecosystem, the LAI could explain 32.5% of the NEE variation (Fig. 6) and the result was higher than that of a temperate desert steppe (26%, Yang *et al*., 2011). This finding is attributed to the additional precipitation received during the plant growing season by the pasture ecosystem.

Diurnal and seasonal variation in NEE: At various stages during the growing season, the carbon absorption of the pasture ecosystem before noon was significantly stronger than the absorption at noon. This type of asymmetric distribution in the daily NEE variation illustrates that the carbon absorption of the pasture ecosystem is significantly suppressed around noon (Fig. 2d). Fu *et al*. (2006) also obtained a similar asymmetrical distribution of NEE from a study of an alpine shrub. Because of photosynthetic depression at high temperatures as well as stomatal closure at high PPFD levels, carbon assimilation was seriously restricted at noon and during the early afternoon. For most plants on the Qinghai-Tibetan Plateau, the photosynthetic depression at noon is a common phenomenon. This response of the plants is primarily due to enhanced respiration and depressed photosynthesis at high temperatures under high radiation conditions (Fu *et al*., 2006).

For the pasture ecosystem, the magnitude of the maximum hourly NEE was -7.89 μmol/CO_2/m^2/sec and this value was lower than that of other grassland ecosystems located at similar latitudes for example, tall prairie

grassland native to North America (-23 μmol/CO_2/m^2/sec) (Ham and Knapp, 1998), the southern plains prairie in the USA (from -9.1 to -15.5 μmol/CO_2/m^2/sec) (Sims and Bradford, 2001), the alpine meadow at Haibei station (-10.8 μmol/CO_2/m^2/sec) (Kato *et al*., 2004). These traits are attributed to the relatively low temperature and vegetation primarily composed of C3 plants in the pasture ecosystem.

For the pasture ecosystem, the magnitude of the maximum daily NEE is -2.91 g/cm^2/day which is located at lower end of the maximum daily NEE variation range (from -1.91 to -9.3 g/cm^2/day) for other artificial grassland ecosystems (Li *et al*. 2005). These data are related to the single sowing method which greatly reduces the plant diversity (Wu *et al*., 2010). Naeem *et al*. (1994) found that the reduction in plant diversity can cause a plant colony's canopy structures to be simplified, reduce their light acquisition and utilization efficiency and therefore reduce their CO_2 uptake of the overall ecosystem.

For annual NEE of the pasture, the pasture in 2008 had medium carbon sink, compared with other carbon sink reports of grassland ecosystem (from -18 to -274 g/cm^2/year) (Li *et al*., 2005). Low air temperature climate and corresponding cool-adapted vegetation characteristics (e.g., the depression of NEE at relatively higher temperatures) might be the main environmental constraints for the carbon sink strength in the pasture.

CONCLUSION

Researchers have adopted eddy covariance to investigate the Net Ecosystem CO_2 Exchange (NEE) for a single-sowed artificial pasture of *Elymus nutans* in TRSR in 2008. The results show that for the pasture, the maximum daily NEE was -2.91 g/cm^2/day and the NEE for the whole year was 140.01 g/cm^2/year. Therefore, the artificial grassland was a carbon sink during 2008. There was a strong biophysical regulation of the NEE during the entire growing season. During the daytime, the NEE was primarily regulated by the PPFD; at night, the NEE was mainly regulated by the T_s. A relatively higher temperature can suppress the photosynthesis of the artificial grassland and it can reduce the carbon absorption capability of the artificial grassland ecosystem. The daily NEE and LAI have a linear relation and 32.5% of the NEE variation can be interpreted by the LAI variation.

ACKNOWLEDGEMENT

This research was supported by the National Natural Science Foundation (31070433) and the Japan-China Research Cooperative Program (2010DFA31290).

REFERENCES

Adams, J.M., H. Faure, L. Faure-Denard, J.M. McGlade and F.I. Woodward, 1990. Increases in terrestrial carbon storage from the last glacial maximum to the present. Nature, 348: 711-714.

Baldocchi, D.D. and P.C. Harley, 1995. Scaling carbon dioxide and water vapour exchange from leaf to canopy in a deciduous forest. II. Model testing and application. Plant Cell Environ., 18: 1157-1173.

Chen, G.M., 2005. The status of the degraded pasture and its strategies of management in black beach of the headwater region of the three river. J. Sichuan Grassland, 10: 37-44.

Davidson, E.A., L.V. Verchot, J.H. Cattanio, I.L. Ackerman and J.E.M. Carvalho, 2000. Effects of soil water content on soil respiration in forests and cattle pastures of Eastern Amazonia. Biogeochemistry, 48: 53-69.

Falge, E., D. Baldocchi, R. Olson, P. Anthoni and M. Aubinet *et al*., 2001. Gap filling strategies for defensible annual sums of net ecosystem exchange. Agric. For. Meteorol., 107: 43-69.

Fang, C. and J.B. Moncrieff, 2001. The dependence of soil CO_2 efflux on temperature. Soil Biol. Biochem., 33: 155-165.

Feng, S., M.C. Tang and D.M. Wang, 1998. New evidence for the Qinghai-Tibetan Plateau as promoter region of climate change in our country. Chin. Sci. Bull., 43: 633-636.

Fu, Y., Z. Zheng, G. Yu, Z. Hu and X. Sun *et al*., 2009. Environmental influences on carbon dioxide fluxes over three grassland ecosystems in China. Biogeosciences, 6: 2879-2893.

Fu, Y.L., G.R. Yu, X.M. Sun, Y.N. Li and X.F. Wen *et al*., 2006. Depression of net ecosystem CO_2 exchange in semi-arid *Leymus chinensis* steppe and alpine shrub. Agric. For. Meteorol., 137: 234-244.

Gu, S., Y. Li, X. Zhao, Y. Tang, M. Du, X. Cui and T. Kato, 2005. Effects of temperature on CO_2 exchange between the atmosphere and an alpine meadow. Phyton-Annales Rei Botanicae, 45: 361-370.

Gu, S., Y. Tang, M. Du, T. Kato, Y. Li, X. Cui and X. Zhao, 2003. Short-term variation of CO_2 flux in relation to environmental controls in an alpine meadow on the Qinghai-Tibetan Plateau. J. Geophys. Res., 108: 4670-4679.

Ham, J.M. and A.K. Knapp, 1998. Fluxes of CO_2, water vapor and energy from a prairie ecosystem during the seasonal transition from carbon sink to carbon source. Agric. For. Meteorol., 89: 1-14.

Hao, Y.B., Y.F. Wang, X.M. Sun, X.Z. Huang and X.Y. Cui *et al*., 2006. Seasonal variation in carbon exchange and its ecological analysis over *Leymus chinensis* steppe in Inner Mongolia. Sci. China Ser. D: Earth Sci., 49: 186-195.

Hunt, J.E., F.M. Kelliher, T.M. McSeveny and J.N. Byers, 2002. Evaporation and carbon dioxide exchange between the atmosphere and a tussock grassland during a summer drought. Agric. For. Meteorol., 111: 65-82.

Jia, B.R., G.S. Zhou and W.P. Yuan, 2007. Modeling and coupling of soil respiration and soil water content in fenced *Leymus chinensis* steppe, Inner Mongolia. Ecol. Modell., 201: 157-162.

Kato, T., Y.H. Tang, S. Gu, X.Y. Cui and M. Hirota *et al*., 2004. Carbon dioxide exchange between the atmosphere and an alpine meadow ecosystem on the Qinghai-Tibetan Plateau, China. Agric. For. Meteorol., 124: 121-134.

Kura-Hotta, M., K. Satoh and S. Katoh, 1987. Relationship between photosynthesis and chlorophyll content during leaf senescence of rice seedlings. Plant Cell Physiol., 28: 1321-1329.

Li, S.G., J. Asanuma, W. Eugster, A. Kotani and J.J. Liu *et al*., 2005. Net ecosystem carbon dioxide exchange over grazed steppe in Central Mongolia. Global Change Biol., 11: 1941-1955.

Lloyd, J. and J.A. Taylor, 1994. On the temperature dependence of soil respiration. Funct. Ecol., 8: 315-323.

McFadden, J.P., W. Eugster and F.S. Chapin III, 2003. A regional study of the controls on water vapor and CO_2 exchange in arctic tundra. Ecology, 84: 2762-2776.

Naeem, S., L.J. Thompson, S.P. Lawler, J.H. Lawton and R.M. Woodfin, 1994. Declining biodiversity can alter the performance of ecosystem. Nature, 368: 734-737.

Novick, K.A., P.C. Stoy, G.G. Katul, D.S. Ellsworth, M.B.S. Siqueira, J. Juang and R. Oren, 2004. Carbon dioxide and water vapor exchange in a warm temperate grassland. Oecologia, 138: 259-274.

Ogren, E., 1993. Convexity of the photosynthetic light-response curve in relation to intensity and direction of light during growth. Plant Physiol., 101: 1013-1019.

Potvin, C., J.P. Simon and B.R. Strain, 1986. Effect of low temperature on the photosynthetic metabolism of the C_4 grass *Echinochloa crus-galli*. Oecologia, 69: 499-506.

Raich, J.W. and W.H. Schlesinger, 1992. The global carbon dioxide flux in soil respiration and its relationship to vegetation and climate. Tellus B, 44: 81-99.

Reichstein, M., J.D. Tenhunen, O. Roupsard, J.M. Ourcival and S. Rambal *et al*., 2002. Severe drought effects on ecosystem CO_2 and H_2O fluxes at three Mediterranean evergreen sites: Revision of current hypotheses? Global Change Biol., 8: 999-1017.

Saito, M., T. Kato and Y.H. Tang, 2009. Temperature controls ecosystem CO_2 exchange of an alpine meadow on the Northeastern Tibetan Plateau. Global Change Biol., 15: 221-228.

Shi, P.L., X.M. Sun, L.L. Xu, X.Z. Zhang, Y.T. He, D.Q. Zhang and G.R. Yu, 2006. Net ecosystem CO_2 exchange and controlling factors in a steppe: *Kobresia* meadow on the Tibetan Plateau. Sci. China Ser. D: Earth Sci., 49: 207-218.

Sims, P.L. and J.A. Bradford, 2001. Carbon dioxide fluxes in a Southern plains prairie. Agric. For. Meteorol., 109: 117-134.

Souza, R.P., E.C. Machado, J.A.B. Silva, A.M.M.A. Lagoa and J.A.G. Silveira, 2004. Photosynthetic gas exchange, chlorophyll fluorescence and some associated metabolic changes in cowpea (*Vigna unguiculata*) during water stress and recovery. Environ. Exp. Bot., 51: 45-56.

Wang, Q.J., D.Z. Lai, Z.C. Jing, S.X. Li and H.L. Shi, 2005. The resources, ecological environment and sustainable development in the source regions of the Yangtze, Huanghe and Yalu Tsangpo rivers. J. Lanzhou Univ. (Nat. Sci.), 41: 50-55.

Wang, W. and J.Y. Fang, 2007. Soil respiration and the effects of human activities in global grasslands. Proceedings of the 3rd EcoSummit 2007-Ecological Complexity and Sustainability: Challenges and Opportunities for 21st-Century Ecology, May 22-27, 2007, Beijing, China, pp: 326-327-.

Wang, Y., G. Zhou and Y. Wang, 2008. Environmental effects on net ecosystem CO_2 exchange at half-hour and month scales over *Stipa krylovii* steppe in Northern China. Agric. For. Meteorol., 148: 714-722.

Webb, E.K., G.I. Pearman and R. Leuning, 1980. Correction of flux measurements for density effects due to heat and water vapour transfer. Q. J. R. Meteorol. Soc., 106: 85-100.

Wilson, K., A. Goldstein, E. Falge, M. Aubinet and D. Baldocchi *et al*., 2002. Energy balance closure at FLUXNET sites. Agric. For. Meteorol., 113: 223-243.

Wohlfahrt, G., M. Anderson-Dunn, M. Bahn, M. Balzarolo and F. Berninger *et al*., 2008. Biotic, abiotic and management controls on the net ecosystem CO_2 exchange of European mountain grassland ecosystems. Ecosystems, 11: 1338-1351.

Wu, G.L., Z.H. Liu, L. Zhang, T.M. Hu and J.M. Chen, 2010. Effects of artificial grassland establishment on soil nutrients and carbon properties in a black-soil-type degraded grassland. Plant Soil, 333: 469-479.

Xu, L.K. and D.D. Baldocchi, 2004. Seasonal variation in carbon dioxide exchange over a Mediterranean annual grassland in California. Agric. For. Meteorol., 123: 79-96.

Yang, F.L., G.S. Zhou, J.E. Hunt and F. Zhang, 2011. Biophysical regulation of net ecosystem carbon dioxide exchange over a temperate desert steppe in Inner Mongolia, China. Agric. Ecosyst. Environ., 142: 318-328.

Yu, G.R. and X.M. Sun, 2006. Principles of Flux Measurement in Terrestrial Ecosystems. Higher Education Press, Beijing, China, pp: 25-78.

Zhao, L., S. Gu, H.K. Zhou, S.X. Xu, X.Q. Zhao and Y.N. Li, 2008. CO_2 fluxes of artificial grassland in the source region of the three rivers on the Qinghai-Tibetan Plateau, China. J. Plant Ecol., 32: 544-554.

Zheng, Z.M., G.R. Yu, Y.L. Fu, Y.S. Wang, X.M. Sun and Y.H. Wang, 2009. Temperature sensitivity of soil respiration is affected by prevailing climatic conditions and soil organic carbon content: A trans-China based case study. Soil Biol. Biochem., 41: 1531-1540.